

## Quasiparticle Relaxation Dynamics in Heavy Fermion Compounds

J. Demsar,<sup>1</sup> R. D. Averitt,<sup>1</sup> K. H. Ahn,<sup>1</sup> M. J. Graf,<sup>1</sup> S. A. Trugman,<sup>1</sup> V. V. Kabanov,<sup>2</sup> J. L. Sarrao,<sup>1</sup> and A. J. Taylor<sup>1</sup>

<sup>1</sup>*Los Alamos National Laboratory, Mail Stop K764, Los Alamos, New Mexico 87545, USA*

<sup>2</sup>*J. Stefan Institute, Jamova 39, SI-1000, Ljubljana, Slovenia*

(Received 11 February 2003; published 8 July 2003)

We present the first femtosecond studies of electron-phonon ( $e$ -ph) thermalization in heavy-fermion compounds. The  $e$ -ph thermalization time  $\tau_{ep}$  increases below the Kondo temperature by more than 2 orders of magnitude as  $T = 0$  K is approached. Analysis using the two-temperature model and numerical simulations based on Boltzmann's equations suggest that this anomalous slowing down of the  $e$ -ph thermalization derives from the large electronic specific heat and the suppression of scattering between heavy electrons and phonons.

DOI: 10.1103/PhysRevLett.91.027401

PACS numbers: 78.47.+p, 71.27.+a

Recent experiments have demonstrated that femtosecond time-resolved optical spectroscopy is a sensitive tool to probe the low-energy electronic structure of strongly correlated electron systems [1–4], complementing conventional time-averaged frequency-domain methods. In these experiments, a femtosecond laser pulse excites a nonthermal electron distribution. This nonthermal distribution rapidly thermalizes through electron-electron ( $e$ - $e$ ) interactions resulting in a change in the occupied density of states (DOS) in proximity to the Fermi energy ( $E_F$ ). Therefore, by measuring photoinduced (PI) reflectivity or transmissivity dynamics as a function of temperature ( $T$ ), it is possible to sensitively probe the nature of the electronic ground state. For example, femtosecond measurements of the carrier relaxation dynamics of high- $T_c$  superconductors and charge density wave compounds have provided new insights into the low-energy electronic structure of these materials [1–3]. What is particularly important is that even though the probe photon wavelength in these experiments ranges from the far-infrared [3] up to several eV [4], the relaxation dynamics on identical samples is the same [3], supporting the basic idea [1] that dynamic PI reflectivity measurements, in many instances, probe relaxation and recombination processes of quasiparticles in the vicinity of  $E_F$ .

In this Letter, we present the first studies of carrier relaxation dynamics in heavy-fermion (HF) compounds using femtosecond time-resolved optical spectroscopy, aiming to elucidate the effect of localized  $f$  electrons [5] on the quasiparticle relaxation dynamics. We have measured the time-resolved PI reflectivity  $\Delta R/R$  dynamics as a function of  $T$  on the series of HF compounds  $\text{YbXCu}_4$  ( $X = \text{Ag, Cd, In}$ ) [6] in comparison to their nonmagnetic counterparts  $\text{LuXCu}_4$ . Our results reveal that the carrier relaxation dynamics are extremely sensitive to the low-energy DOS near  $E_F$ . In particular, in HF compounds the relaxation time  $\tau_r$  shows a hundredfold increase between the Kondo temperature ( $T_K$ ) and 10 K, while in the nonmagnetic analogues  $\tau_r$  is nearly constant, similar to conventional metals such as Ag, Au, and Cu [7]. Our analysis shows that the relaxation dynamics can

be attributed to  $e$ -ph thermalization and that the anomalous slowing down of the  $e$ -ph thermalization stems from the large electronic specific heat in HF compounds and suppression of  $e$ -ph scattering within the peak in the enhanced DOS near  $E_F$ .

In the following, we focus on  $\text{YbAgCu}_4$  (a prototypical HF system with  $T_K \sim 100$  K and low- $T$  Sommerfeld coefficient  $\gamma \sim 210$  mJ/mol K<sup>2</sup>) [6] compared to its nonmagnetic counterpart  $\text{LuAgCu}_4$  ( $\gamma \sim 10$  mJ/mol K<sup>2</sup>). The experiments were performed on freshly polished flux-grown single crystals [6]. We used a standard pump-probe setup with a mode-locked Ti:sapphire laser producing 20 fs pulses centered at 800 nm (photon energy  $\hbar\omega_{\text{ph}} \simeq 1.5$  eV) with an 80 MHz repetition rate. The PI changes in reflectivity  $\Delta R/R$  were measured using a photodiode and lock-in detection. The pump fluence was kept below  $0.1 \mu\text{J}/\text{cm}^2$  to minimize the overall heating of the illuminated spot [8], while the pump/probe intensity ratio was  $\sim 30$ . Steady-state heating effects were accounted for as described in [8], yielding an uncertainty in  $T$  of  $\pm 3$  K (in all the data the  $T$  increase of the illuminated spot has been accounted for).

Figure 1 presents the PI reflectivity traces on the two compounds at several  $T$  between  $\approx 10$  and 300 K. The

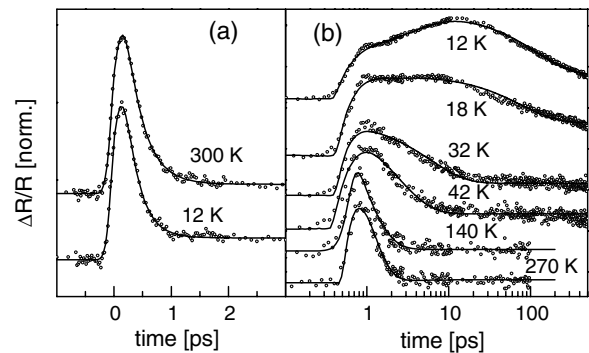


FIG. 1. Normalized PI reflectivity data (solid symbols) on (a)  $\text{LuAgCu}_4$  and (b)  $\text{YbAgCu}_4$  at various  $T$ , together with best fits (see text) to the data—solid lines. The data have been vertically shifted for clarity.

relaxation dynamics of the non-HF compound LuAgCu<sub>4</sub> display a very weak  $T$  dependence, with  $\Delta R/R$  recovering on a subpicosecond time scale at all  $T$ . The dynamics are similar to regular metals such as Au and Ag [7], where the recovery is predominantly due to  $e$ -ph thermalization. In contrast, Fig. 1(b) shows that for YbAgCu, the quasiparticle dynamics are strongly  $T$  dependent. Specifically, above  $\sim 140$  K, the recovery time  $\tau_r$  [determined by an  $\exp(-t/\tau_r)$  fit to the data] is virtually  $T$  independent but increases by more than 2 orders of magnitude as  $T \rightarrow 0$  K. We have measured similar dynamics on YbCdCu<sub>4</sub> ( $T_K \sim 100$  K,  $\gamma \sim 200$  mJ/mol K<sup>2</sup>). Furthermore, a similar divergence of  $\tau_r$  occurs for CeCoIn<sub>5</sub> below  $\approx 60$  K, implying that the observed increase in the relaxation time starting at  $\sim T_K$  and its subsequent divergence as  $T \rightarrow 0$  K is a generic feature of HF compounds and derives from their low-energy electronic structure.

The rise-time dynamics are also different in the two compounds. For LuAgCu<sub>4</sub>, the rise time is  $\sim 100$  fs at all  $T$ . This is again similar to what has been measured on conventional metals and reflects the time it takes for the initially created high energy quasiparticles to thermalize towards  $E_F$ . Above  $\sim 25$  K, YbAgCu<sub>4</sub> displays a similar (fast) rise time. Below 25 K the rise time increases and, as the semilog plot in Fig. 1(b) reveals, becomes two exponential at the lowest  $T$ . Similar behavior also occurs for CeCoIn<sub>5</sub>, but is absent in YbCdCu<sub>4</sub> indicating a strong dependence on the details of the low-energy electronic structure in HF compounds. While noting the presence of these anomalous rise-time dynamics, further systematic studies are needed to obtain a more complete understanding [9]. In the following, we focus on the anomalous  $T$  dependence of recovery dynamics below  $T_K$  which seem to be a general feature of HF compounds.

In conventional metals, the initial PI change in the reflectivity arises from changes in occupation near  $E_F$  after  $e$ - $e$  thermalization. Subsequently, the PI reflectivity recovery dynamics proceed on a picosecond time scale governed by  $e$ -ph thermalization [7]. The two-temperature model (TTM) serves as a useful starting point in describing  $e$ -ph thermalization in metals [10–12]. The TTM describes the time evolution of the electron ( $T_e$ ) and lattice ( $T_l$ ) temperatures by two coupled differential equations [7,10]. In the low photoexcitation energy density limit, as in our case, when  $T_e - T_l \ll T_l$  over the entire  $T$  range, the set of two coupled differential equations can be linearized, resulting in the following expression for the  $e$ -ph thermalization time:

$$\tau_{ep}^{-1} = g(C_e^{-1} + C_l^{-1}). \quad (1)$$

Here  $C_e$  and  $C_l$  are the electronic and lattice specific heats, respectively, and  $g(T_l)$  is the  $e$ -ph coupling function [7,10]. In the case of simple metals, when the electron bandwidth is much larger than the Debye energy  $\hbar\omega_D = k_B\Theta_D$ , and using the Debye model for the  $e$ -ph interaction,  $g(T)$  has particularly simple form. It is given by

$g(T) = dG(T)/dT$ , where [7,11]

$$G(T) = 4g_\infty \left(\frac{T}{\Theta_D}\right)^5 \int_0^{\Theta_D/T} dx \frac{x^4}{e^x - 1} \chi(x, T). \quad (2)$$

Here  $g_\infty$  is termed the  $e$ -ph coupling constant, while  $\chi(x, T)$  is included to account for the variation in the electronic DOS  $D_e(\epsilon)$  and the normalized  $e$ -ph scattering strength  $F(\epsilon, \epsilon')$ , over the energy range  $E_F \pm \hbar\omega_D$ . It can be shown using Fermi's golden rule that

$$\chi(x, T) = \frac{1}{\xi} \int_{-\infty}^{\infty} d\epsilon \frac{D_e(\epsilon)D_e(\epsilon')F(\epsilon, \epsilon')}{D_0^2} \{f_0(\epsilon) - f_0(\epsilon')\}, \quad (3)$$

where  $\epsilon' = \epsilon + \xi$ , and  $\xi = xT$  and  $f_0$  is the Fermi-Dirac distribution. In metals such as Au or Ag,  $D_e(\epsilon)$  and  $F$  are approximately constant in this energy range, i.e.,  $D_e(\epsilon) = D_0$  and  $F = 1$ , giving  $\chi \equiv 1$ .  $g_\infty$  is typically  $10^{15}$ – $10^{16}$  W/mol K [e.g., for Cu  $g_\infty = 6.2 \times 10^{15}$  W/mol K corresponding to  $g(300 \text{ K}) = 1 \times 10^{17}$  W/m<sup>3</sup> K [13]].

At  $T > \Theta_D$ ,  $\tau_{ep}(T)$  given by the TTM has been found to describe the temperature as well as photoexcitation intensity dependence of measured  $\tau_r(T)$  [7,13]. Moreover, since the absolute value of  $\tau_{ep}$  is determined by a single parameter  $g_\infty$ , the technique has been successfully used to determine the dimensionless  $e$ -ph coupling constants  $\lambda$  in superconductors [12,14]. However, at low  $T$  ( $T \lesssim \Theta_D/5$ ), the TTM prediction of  $\tau_{ep} \propto T^{-3}$  has never been observed in metals [7]—instead,  $\tau_r$  saturates at a constant value at low  $T$ . The discrepancy between the experimental results and the TTM was found to be due to the fact that the TTM neglects  $e$ - $e$  thermalization processes (by implicitly assuming that a Fermi-Dirac distribution is created instantly following photoexcitation). From simulations using coupled Boltzmann equations, Groeneveld *et al.* [7] showed that this discrepancy is due to the fact that at low  $T$  the  $e$ - $e$  and  $e$ -ph thermalization times are comparable. Since  $\tau_{ep} \propto T$  above  $\approx \Theta_D/5$  [7,12], while  $\tau_{ee} \propto T^{-2}$ —see Eq. (16) of Ref. [7], the TTM is expected to fail at low  $T$  where  $\tau_{ee} \gtrsim \tau_{ep}$ .

In Fig. 2 we plot the  $T$  dependence of  $\tau_r$  on LuAgCu<sub>4</sub> (solid circles), together with the TTM prediction for  $\tau_{ep}$  (dashed line) given by Eqs. (1) and (2) with  $\Theta_D = 280$  K [6], measured  $C_e(T)$  and  $C_l(T)$ —see inset in Fig. 2, and  $g_\infty = 2.6 \times 10^{15}$  W/mol K. Similar to Au or Ag [7], we find good agreement at  $T \gtrsim 200$  K, while below 40 K instead of showing a  $\tau_{ep} \propto T^{-3}$  divergence,  $\tau_r$  saturates.

In order to explain the discrepancy, we have carried out numerical simulations using coupled Boltzmann equations [7,15]. Here, for example, the net phonon absorption by electrons with energy  $\epsilon$  is represented by  $[df_\epsilon/dt]_{ep}^{abs} = \int d\omega K_{ep} S(\epsilon, \omega) D_p(\omega) D_e(\epsilon + \omega)$ , where  $D_e(\epsilon)$  and  $D_p(\omega)$  are the electron and phonon DOS, and  $S(\epsilon, \omega) = f_{\epsilon+\omega}(1 - f_\epsilon) - b_\omega(f_\epsilon - f_{\epsilon+\omega})$ , with  $f$  and  $b$  being the electron and phonon distribution functions, respectively.  $K_{ep}$  in the above equation and  $K_{ee}$  in  $e$ - $e$  scattering represent the square of the scattering matrix

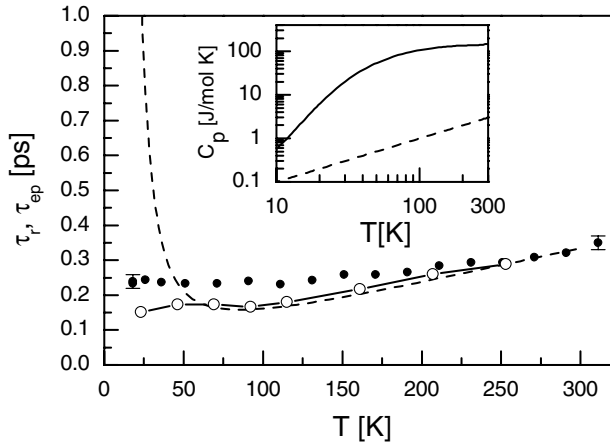


FIG. 2. (a)  $T$  dependence of relaxation time  $\tau_r$  on LuAgCu<sub>4</sub> (solid circles), together with the TTM prediction (dashed line) and the result of the numerical simulation (open circles) including the nonthermal electron distribution. Inset:  $C_e$  (dashed line) and  $C_l$  (solid line) of LuAgCu<sub>4</sub>.

element, combined with all other numerical factors [7,15]. When performing numerical simulations, a thermal phonon distribution [ $b_{l=0} = b_0(T_l)$ ] and a nonthermal electron distribution [ $f_{l=0} = f_0(T_e) \pm \delta f$ ] was taken as the initial condition just after the laser pulse [7], while  $\tau_{ep}$  is found by fitting the total electron energy versus time curve to an exponential decay function. The initial perturbation  $\delta f$  is around  $10^{-5}$ – $10^{-3}$  for the energy range between 0.10–0.15 eV above and below  $E_F$ , which is small enough that the increase in  $T$  after  $e$ -ph thermalization is less than 1 K over the whole  $T$  range—consistent with the small excitation intensity used in the experiment [16]. The phonon and electron DOS used in the simulation were chosen such that they fit the specific heat data [i.e., for the phonon DOS, we use the Debye model  $D_p(\omega) \sim \omega^2$  with  $\hbar\omega_D = 24$  meV, while  $D_e(E_F) \approx 2.1$  eV<sup>-1</sup> f.u.<sup>-1</sup> spin<sup>-1</sup>]. The result of the simulation using the absolute value of  $K_{ep} = 0.93$  ps<sup>-1</sup> eV and  $K_{ee}/K_{ep} = 700$  is plotted by open circles [17] in Fig. 2. As expected, the simulation gives the same result as the TTM at high  $T$ , while at low temperatures  $\tau_{ep}$  saturates in agreement with the experimental  $\tau_r$ .

Figure 3 shows  $\tau_r(T)$  obtained on YbAgCu<sub>4</sub>. At  $T > T_K$  the value of  $\tau_r$  is similar to LuAgCu<sub>4</sub>. At low  $T$ , however,  $\tau_r$  increases by more than 2 orders of magnitude. Since heavy fermions are characterized by a peak in the DOS at  $E_F$  [5], the appropriate  $D_e(\epsilon)$  should be used when modeling  $\tau_{ep}(T)$ . In our calculation we used  $D_e(\epsilon) = D_{\text{peak}} \exp[-(\epsilon/\Delta)^2] + D_0$ , where  $D_{\text{peak}} = 70$  eV<sup>-1</sup> f.u.<sup>-1</sup> spin<sup>-1</sup>,  $\Delta = 13$  meV, and  $D_0 = 2.1$  eV<sup>-1</sup> f.u.<sup>-1</sup> spin<sup>-1</sup> (identical to the value for LuAgCu<sub>4</sub>). It reproduces the experimental  $T$  dependence of  $C_e$ , as shown in the inset in Fig. 3. For simplicity we choose  $E_F$  at the center of the peak, so that the chemical potential is constant. Since  $D_e(E_F)$  is almost 2 orders of magnitude larger than in LuAgCu<sub>4</sub> we expect that the  $e$ -

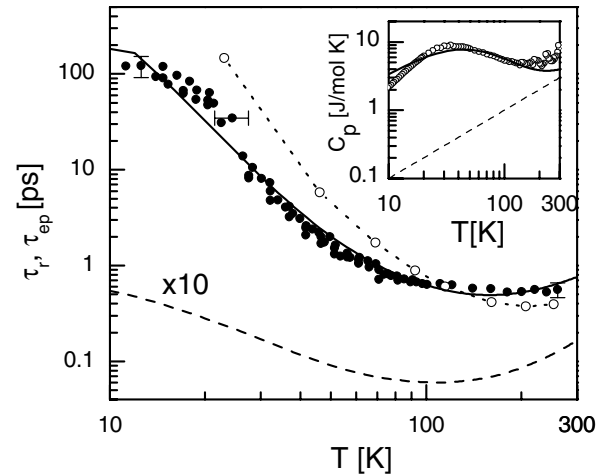


FIG. 3.  $T$  dependence of  $\tau_r$  on YbAgCu<sub>4</sub> (solid circles), together with the corresponding  $\tau_{ep}$  (multiplied by 10 for presentation purposes) from simple TTM prediction (dashed line). Assuming suppressed scattering of heavy electrons by phonons due to  $v_F < v_s$  condition, very good agreement with the data is obtained: open circles present the result of numerical simulation, while solid line presents the TTM simulation—see text. Inset: experimentally determined  $C_e(T)$  for YbAgCu<sub>4</sub> (open circles), together with calculated  $C_e(T)$  based on the model  $D_e(\epsilon)$ —solid line.  $C_e(T)$  of LuAgCu<sub>4</sub> (dashed line) is added for comparison.

thermalization is much faster in YbAgCu<sub>4</sub> and that the TTM would be valid at the lowest  $T$ .

The calculated  $\tau_{ep}(T)$  using Eq. (2) is plotted in Fig. 3 by the dashed line. Here the approximate  $C_e(T)$  and  $C_l(T)$  were used,  $g_\infty$  was taken to be the same as for LuAgCu<sub>4</sub>, while  $\chi(x, T)$  was evaluated explicitly for the above  $D_e(\epsilon)$  and  $F = 1$ . Since  $\tau_{ep}^{-1} \propto D_e$ , and  $D_e(E_F) \gg D_0$ , the result is not surprising, implying that the simple TTM cannot account for the observed dramatic increase in  $\tau_r$  at low  $T$ . We should note that neither the value of the  $e$ -ph coupling constant  $g_\infty$  nor  $D_0$ , which determine the absolute value of  $\tau_{ep}$ , are necessarily the same in YbXCu<sub>4</sub> and LuXCu<sub>4</sub>. However, even if the  $e$ -ph coupling is 10 times smaller in YbAgCu<sub>4</sub> compared to LuAgCu<sub>4</sub> (which would give a 10 times larger value of  $\tau_{ep}$ —as plotted by dashed line in Fig. 3), the observed  $T$  dependence of  $\tau_r$  still cannot be accounted for.

In order to account for the observed  $\tau_r(T)$  we have to consider the nature of the electronic states within the peak in the DOS. In heavy fermions the peak in  $D_e(\epsilon)$  originates from hybridization of the localized  $f$  levels with the conduction band electrons [5]. We hypothesize that the  $e$ -ph scattering within the DOS peak is suppressed, since the band dispersion near  $E_F$  is much weaker than in regular metals. Therefore, it is quite possible that the Fermi velocity  $v_F$  is smaller than the sound velocity  $v_s$ , in which case *momentum and energy conservation* prohibit  $e$ -ph scattering when both initial and final electron states lie within the energy range where  $v_F < v_s$ . Assuming a parabolic band with  $E_F \sim T_K \sim$

100 K, and 0.85 carriers per formula unit [18], one obtains  $v_F \sim 4$  km/sec, while the longitudinal sound velocity for  $\text{YbIn}_{1-x}\text{Ag}_x\text{Cu}_4$  ( $x < 0.3$ ) is  $\approx 4.4$  km/sec along [111] direction [19] (similar  $v_s$  is expected for  $\text{YbAgCu}_4$ ). Even though a parabolic dispersion relation is just a rough approximation, and a direct measurement such as the de Haas–van Alphen effect is required to obtain  $v_F$ , our simple estimate supports this idea.

Using this hypothesis, good agreement with the data can be obtained.  $\tau_{ep}(T)$  obtained by numerical simulations based on Boltzmann equations with  $K_{ep}$  set to 0 for processes where the initial and final electronic state are in the range of  $-24 < \epsilon < 24$  meV (i.e., within the DOS peak), and  $K_{ep} = 0.23 \text{ ps}^{-1} \text{ eV}$  otherwise, is plotted by open circles in Fig. 3. Even better agreement with the data is obtained from the TTM, assuming that the  $e$ -ph interaction strength  $F(\epsilon, \epsilon')$  entering Eq. (3) smoothly vanishes as  $\epsilon$  and  $\epsilon' \rightarrow E_F$ , accounting for  $v_F$  variation (and thus  $v_F < v_s$  condition) across the Fermi surface. This is implemented into the TTM simulation by approximating the factor  $D_e(\epsilon)D_e(\epsilon')F(\epsilon, \epsilon')$  in Eq. (3) with the symmetrized function  $[D_e(\epsilon)D_{ie}(\epsilon') + D_e(\epsilon')D_{ie}(\epsilon) - D_{ie}(\epsilon)D_{ie}(\epsilon')]$ , where  $D_{ie}(\epsilon) = D_0 - D_0 \exp[-(\epsilon/\Delta')^2]$ . The resulting  $\tau_{ep}(T)$ , using  $\Delta' = 24$  meV, and  $g_\infty = 4.5 \times 10^{14} \text{ W/mol K}$  is plotted by the solid line in Fig. 3. Indeed, extremely good agreement with the data is obtained, even though  $\tau_r$  spans more than 2 orders of magnitude [20].

With the hypothesis that  $e$ -ph scattering is suppressed in the DOS peak, the experimental observation of anomalous  $T$  dependence of  $\tau_r$  can be understood. Namely, at  $T < T_K$   $C_e(T)$  increases dramatically compared to normal metals. On the other hand,  $e$ -ph relaxation becomes more and more difficult as  $T$  is lowered since most of the electron relaxation should occur within the DOS peak, where the  $e$ -ph scattering is blocked by *energy and momentum* conservation. Therefore, the thermalization between electrons and the lattice occurs very slowly, giving rise to the divergent  $\tau_{ep}$  below  $T_K$ .

While the presented model explains the main features of the data, i.e., the low- $T$  divergence of  $\tau_{ep}$ , there are still several issues requiring further experimental and theoretical effort. For example, in the simulations we considered a  $T$ -independent peak in the DOS, assuming that many-body and correlation effects can be described by effective,  $T$ -independent model parameters. This may be an oversimplification of the physics of heavy-fermion systems. However, the relaxation time simulations and specific heat calculations of our phenomenological model depend only weakly on a  $T$ -dependent DOS, as long as the peak width in the DOS does not vary faster than  $T$ . Further, it would be interesting to investigate  $e$ -ph thermalization in Kondo insulators. Namely, due to the presence of the gap near  $E_F$  one would expect effects similar to the Rothwarf-Taylor bottleneck observed in superconductors [1]. Second, even more interesting effects are expected due to the strong reduction of the screening at

low frequencies (below the gap) which could lead to nonadiabatic phonons.

In conclusion, we have utilized ultrafast optical spectroscopy to study the dynamics of photoexcited quasiparticles in HF compounds. We have observed a divergence in the  $e$ -ph thermalization time at low  $T$ . We argue that the dramatic hundredfold increase in the relaxation time at low  $T$  in  $\text{YbXCu}_4$  (and the lack of this quasidivergence in the non-HF  $\text{LuXCu}_4$  analogs) results from the largely increased DOS at  $E_F$  coupled with strongly suppressed scattering of heavy electrons by phonons.

We thank Kaden Hazzard for the specific heat data. This work was supported by U.S. DOE.

- 
- [1] V.V. Kabanov *et al.*, Phys. Rev. B **59**, 1497 (1999).
  - [2] J. Demsar *et al.*, Phys. Rev. Lett. **83**, 800 (1999).
  - [3] R. D. Averitt *et al.*, Phys. Rev. B **63**, 140502 (2001).
  - [4] C. J. Stevens *et al.*, Phys. Rev. Lett. **78**, 2212 (1997).
  - [5] A. C. Hewson, *The Kondo Problem to Heavy Fermions* (Cambridge University Press, Cambridge, 1993); L. Degiorgi, Rev. Mod. Phys. **71**, 687 (1999).
  - [6] J. L. Sarrao *et al.*, Phys. Rev. B **59**, 6855 (1999); T. Graf *et al.*, Phys. Rev. B **51**, 15 053 (1995).
  - [7] R. H. M. Groeneveld, R. Sprik, and A. Lagendijk, Phys. Rev. B **51**, 11 433 (1995), and references therein.
  - [8] D. Mihailovic and J. Demsar, in *Spectroscopy of Superconducting Materials*, edited by E. Falques, ACS Symposium Series 730 (The American Chemical Society, Washington, DC, 1999).
  - [9] The anomalous rise-time dynamics may reflect some kind of a bottleneck in the  $e$ - $e$  thermalization due to complicated low-energy electronic structure, e.g., hybridization gap.
  - [10] S. I. Anisimov, B. L. Kapeliovich, and T. L. Perel'man, Sov. Phys. JETP **39**, 375 (1974).
  - [11] M. I. Kaganov, I. M. Lifshitz, and L. V. Tanatarov, Sov. Phys. JETP **4**, 173 (1957).
  - [12] P. B. Allen, Phys. Rev. Lett. **59**, 1460 (1987).
  - [13] H. E. Elsayed-Ali *et al.*, Phys. Rev. Lett. **58**, 1212 (1987).
  - [14] S. D. Brorson *et al.*, Phys. Rev. Lett. **64**, 2172 (1990).
  - [15] K. H. Ahn *et al.* (unpublished).
  - [16] The simulation shows that  $\tau_{ep}$  does not depend on the details of the initial condition [7,15].
  - [17] While  $K_{ee}$  is not uniquely determined, fitting  $\tau_{ep}$  to the experimental data requires  $K_{ee}/K_{ep} < 7 \times 10^3$ . If  $K_{ee}/K_{ep} \geq 7 \times 10^3$  the  $e$ - $e$  scattering rate is fast enough for the electron system to quickly reach thermal distribution, resulting in  $\tau_{ep} \propto T^{-3}$  behavior predicted by the TTM. Indeed, the analysis of the time evolution of  $df/dt$  shows that if  $K_{ee}/K_{ep} = 700$ , then  $\tau_{ee} > \tau_{ep}$  at low  $T$  [15].
  - [18] J. M. Lawrence *et al.*, Phys. Rev. B **63**, 054427 (2001).
  - [19] S. Zherlitsyn *et al.*, Phys. Rev. B **60**, 3148 (1999).
  - [20] The absolute values of the  $e$ -ph coupling in both numerical and the TTM simulations were smaller than the corresponding value for  $\text{LuAgCu}_4$  by about half in terms of the scattering matrix element.